Infrared Spectroscopic Characterization of Cyanocuprates

Hui Huang,[†] Khris Alvarez,[†] Qiang Lui,[‡] Terence M. Barnhart,[†] James P. Snyder,*[,‡] and James E. Penner-Hahn*[,†]

Contribution from The Willard H. Dow Laboratories, Department of Chemistry, The University of Michigan, Ann Arbor, Michigan 48109-1055, and Department of Chemistry, Emory University, Atlanta, Georgia 30329

Received June 3, 1996[⊗]

Abstract: The synthetically useful cyanocuprates MeCu(CN)Li (**2**) and "$Me_2CuLi{\cdot}LiCN$" (**3**) have been characterized by infrared spectroscopy. Titration of $CuCN{\cdot}2LiCl$ (**1**) with MeLi in THF solution has established that **2** has an IR absorption due to cyanide stretching at 2133 cm^{-1} with $\epsilon = 2.3 \times 10^3$ cm^{-2} M^{-1}, while the CN stretching frequency for **3** occurs at 2115 cm^{-1} with $\epsilon = 4.0 \times 10^2$ cm^{-2} M^{-1}. The spectra suggest that **2** and **3** are the only significant cuprate species present in the methylcyanocuprate system. The IR titration data give a formation constant of approximately 8×10^3 for **2** + MeLi ⇌ **3**. The present data stand in contrast to earlier reports that **2** and **3** have identical IR spectra. The earlier conclusion appears to have been a consequence of the significantly different molar absorptivity of cyanide in **2** and **3** and the presence of small amount of **2** in equilibrium with **3** when the MeLi:CuCN ratio is 2:1. *Ab initio* calculations of the frequencies and intensities of the CN stretch are able to semiquantitatively reproduce the observed trends using a model in which the CN^- is bound to the Cu in **2** but is not bound directly to the Cu in **3**. The predicted CN stretch for a "higher order" cyanocuprate structure, with a three-coordinate $[Me_2CuCN]^{2-}$, is not consistent with the observed value. In contrast, the seven-membered bridged Gilman cuprate **14** appears to fulfill all of the structural and IR spectroscopic requirements for the 2115 cm^{-1} species.

Cyanocuprate reagents prepared from the addition of organolithium reagents to a copper(I) salt have proven to be extremely useful alkylation reagents in organic synthesis.[1−3] The organocuprates generated from the addition of 2 equiv of organolithium to CuCN have been found to be particularly useful, frequently giving better yields than the dialkylorganocuprates prepared using copper(I) halides.[4−6] The cyanocuprate reagents have been studied extensively by NMR,[7−11] IR,[7,9,12] and EXAFS[13−15] spectroscopies and by *ab initio* calculations.[15−17] There is general agreement that monoalkylcyanocuprates contain a copper that is linearly coordinated by an alkyl group and a cyanide.[7,10,13,15,16,18] In contrast, the structural understanding of diorganocyanocuprates has been more controversial. The diorganocyanocuprates have been described as "higher order" cyanocuprates, in which the copper is three coordinate with both alkyl and cyanide ligands.[7,9,11,12] More recent studies have suggested instead a structure in which the Cu is directly coordinated to the two alkyl groups, with the cyanide weakly associated with the $[Me_2Cu]^-$ unit.[8,13,14,16,17]

Infrared spectroscopy has been used extensively to study metal cyanides in both solid state and solution[19−22] and has great potential in the structural characterization of cyanocuprates. The cyanide stretch at 2000−2250 cm^{-1} is very sensitive to the cyanide bonding environment,[23] and the cyanide absorption region is readily accessible in most organic solvents.

Previous IR studies of cyanocuprates reported that there was no significant difference in ν_{CN} for methyl- and dimethylcyanocuprate reagents dissolved in diethyl ether,[7] both of which were observed at 2105 cm^{-1}. THF solutions of dimethylcyanocuprate have been reported to have two bands in the ν_{CN} region, either[9] at 2138 cm^{-1} and 2118 cm^{-1} or[12] at 2130 cm^{-1} and 2109 cm^{-1}. In the latter case, the lower frequency band (2109 cm^{-1}) was observed as a shoulder.[12] In the former, a time dependent equilibrium of different dimethylcyanocuprate species was reported to exist at 0 °C.[7] Five minutes after preparation of the dialkylcyanocuprate ($Me_2Cu(CN)Li_2$), both bands were observed, with the 2118 cm^{-1} peak slightly more intense than the 2138 cm^{-1} peak. One hour after preparation, the relative intensities had inverted, and two hours after preparation, the 2138 cm^{-1} peak increased so much that the 2118 cm^{-1} band was negligible. The 2138 cm^{-1} peak was assigned to the stable form of dimethylcyanocuprate.

[†] The University of Michigan.
[‡] Emory University.
[⊗] Abstract published in *Advance ACS Abstracts,* September 1, 1996.

(1) Marino, J. P.; Jaen, J. C. *J. Am. Chem. Soc.* **1982**, *104*, 3165.
(2) Lipshutz, B. H.; Wilhelm, R. S.; Kozlowski, J. A. *Tetrahedron* **1984**, *40*, 5005.
(3) Lipshutz, B. H.; Sengupta, S. *Org. React. (N.Y.)* **1992**, *41*, 135.
(4) Wilhelm, R. S. Ph.D. Thesis, University of California, 1984.
(5) Lipshutz, B. H.; Sengupta, S. *Org. React. (N.Y.)* **1992**, *41*, 219−228.
(6) Bertz, S. H.; Miao, G.; Eriksson, M. *J. Chem. Soc., Chem. Commun.* **1996**, 815.
(7) Lipshutz, B. H.; Kozlowski, J. A.; Wilhelm, R. S. *J. Org. Chem.* **1984**, *49*, 3943.
(8) Bertz, S. H. *J. Am. Chem. Soc.* **1990**, *112*, 4031−4032.
(9) Lipshutz, B. H.; Sharma, S.; Ellsworth, E. L. *J. Am. Chem. Soc.* **1990**, *112*, 4032−4034.
(10) Bertz, S. H. *J. Am. Chem. Soc.* **1991**, *113*, 5470−5471.
(11) Lipshutz, B. H.; James, B. *J. Org. Chem.* **1994**, *59*, 7585.
(12) Singer, R. D.; Oehlschlager, A. C. *J. Org. Chem.* **1992**, *57*, 2192−2195.
(13) Stemmler, T. S.; Penner-Hahn, J. E.; Knochel, P. *J. Am. Chem. Soc.* **1993**, *115*, 348−350.
(14) Barnhart, T. M.; Huang, H.; Penner-Hahn, J. E. *J. Org. Chem.* **1995**, *60*, 4310−4311.
(15) Stemmler, T. L.; Barnhart, T.; Penner-Hahn, J. E.; Tucker, C. E.; Knochel, P.; Böhme, M.; Frenking, G. *J. Am. Chem. Soc.* **1995**, *117*, 12489−12497.
(16) Snyder, J. P.; Spangler, D. P.; Behling, J. R.; Rossiter, B. E. *J. Org. Chem.* **1994**, *59*, 2665−2667.
(17) Snyder, J. P.; Bertz, S. H. *J. Org. Chem.* **1995**, *60*, 4312−4313.
(18) Bertz, S. H.; Dabbagh, G. *J. Chem. Soc., Chem. Commun.* **1982**, 1030.
(19) Penneman, R. A.; Jones, L. H. *J. Chem. Phys.* **1956**, *24*, 293−296.
(20) Dows, D. A.; Haim, A.; Wilmarth, W. K. *J. Inorg. Nucl. Chem.* **1961**, *21*, 33.
(21) Jones, L. H. *Inorg. Chem.* **1963**, *2*, 777−780.
(22) Bignozzi, C. A.; Argazzi, R.; Schoonover, J. R.; Gordon, K. C.; Dyer, R. B.; Scandola, F. *Inorg. Chem.* **1992**, *31*, 5260−5267.
(23) Nakamoto, K. In *Infrared Spectra of Inorganic and Coordination Compounds*, 1st ed.; John Wiley & Sons, Inc.: New York, London, 1963.

S0002-7863(96)01862-8 CCC: $12.00

This interpretation of the IR spectra of the dialkylcyanocuprates suggests that there is no change in ν_{CN} between the mono- and dialkylcyanocuprates. This has been used to argue that cyanide remains bound to Cu in the dialkylcyanocuprates. The latter conclusion is inconsistent with recent EXAFS,[13,15] NMR,[8] and theoretical results,[16,17] each of which has suggested that the cyanide in dialkylcyanocuprates is *not* bonded directly to the copper center. In order to establish the identity of the cyanocuprate species that correspond to the IR absorption bands, we have conducted a combined experimental and theoretical study. A detailed IR titration of the methylcyanocuprate system suggests a reinterpretation of the earlier IR studies. The density functional (DFT) calculations of geometry and CN vibrational frequencies permit explicit structural assignments.

Experimental Section

Sample Preparation. All organocuprate samples were prepared under dry nitrogen using standard Schlenk techniques. LiCl and CuCN (99%) were purchased from Aldrich Chemical Company. The LiCl was dried under vacuum at 150 °C for 2 h before use. CuCN was dried under vacuum at 60 °C for 2 h before use. Halide free organolithium reagents were purchased from Aldrich in Sure/Seal bottles and were titrated with 2-butanol using 1,10-phenanthroline as an indicator immediately prior to use. THF solvent was freshly distilled from Na/benzophenone before use.

The copper concentration was 0.1 M in all cuprate samples at room temperature. The volume decreased by 7% on cooling from room temperature to dry ice temperature, giving final concentrations of 0.108 M at low temperature. A typical procedure was as follows: To prepare [MeCuCN]Li, 25 mL of THF was injected into a clean, dry, septum-sealed 50 mL round bottom Schlenk flask containing 0.42 g (10.0 mmol) of LiCl and a magnetic stir bar. The mixture was stirred until the LiCl dissolved. This solution was then transferred via a stainless steel cannula to a second 50 mL Schlenk flask containing 0.45 g (5.0 mmol) of dry CuCN and was stirred until the CuCN dissolved. Then 2.5 mL of this preformed CuCN·2LiCl solution (0.2 M) was transferred to a 25 mL dry Schlenk flask. Dry THF (2.14 mL) was also injected to this same flask in order to make the final concentration of copper 0.1 M. Upon cooling to −78 °C, 1 equiv of MeLi solution (0.36 mL, 1.40 M in Et_2O) was added via syringe. After 5 min of stirring at −78 °C, the flask was warmed to 0 °C and allowed to stir for 5 min, yielding a clear colorless solution. The flask was then returned to the dry ice/acetone bath.

Infrared Spectroscopy. Infrared spectra were measured on Nicolet 60SX spectrometers with a spectral resolution of 2 cm^{-1}. Samples were quickly cannulated to a SPECAC variable temperature cell, model 21001. CaF_2 plates were used as the windows for the sample cell with either a 200 or 100 μm space between the parallel CaF_2 windows. The spectra were measured both at −78 °C and at room temperature. They are almost the same except that the absorption peaks for the room temperature spectra appear to be shifted by 2−3 cm^{-1} with respect to those for the low temperature ones. Only the spectra measured at −78 °C are presented in this paper.

Data Analysis. Infrared absorption spectra were corrected by subtracting the spectrum for pure THF measured under the same conditions. The absorption spectra were analyzed by fitting each peak with a combination of Gaussian and Lorentzian functions. The 2115 cm^{-1} peak could be fit with a single Gaussian line shape, while the 2150 and 2133 cm^{-1} peaks could only be fit with a mixture of Gaussian and Lorentzian functions. The relative area of the Gaussian and Lorentzian functions was 1:1. The intensity of each peak was obtained by analytical integration of the function that gave the best fit. In subsequent fits to titration data (Figure 2), the center, widths, and relative heights of these functions were held constant.

Ab Initio Computations. All structures reported below were optimized within Gaussian 92 or 94[24] with the LANL2DZ basis set supplemented by the nonlocal density functional B3LYP (B3LYP/LANL2DZ).[25,26] LANL2DZ as incorporated in the Gaussian series of programs employs the Los Alamos 10-electron effective core potential (ECP-2) plus a double-ζ (DZ) basis for copper ((8s2p5d)/[3s2p2d] contraction with (341/311/41) splitting) and utilizes the D95V basis for atoms from H to Ne.[27,28] The normal coordinate analysis was performed with analytical second derivatives using a procedure tailored to organometallic effective core potentials.[29]

(24) GAUSSIAN 92 and 94, Frisch, M. J. et al.; 1992 and 1994.

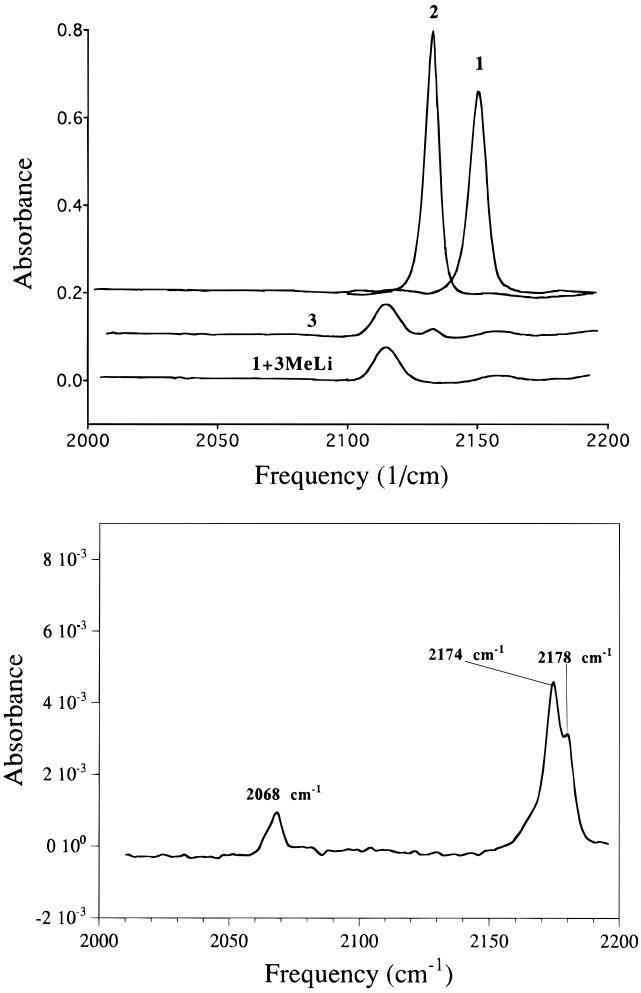

Figure 1. IR spectra of THF solutions of cyanocuprates: (top) CuCN·2LiCl (**1**), CuCN·2LiCl + MeLi (**2**), CuCN·2LiCl + 2MeLi (**3**), and CuCN·2LiCl + 3MeLi; (bottom) LiCN, 5.0 mM solution in THF. All Cu samples were 0.1 M and measured at −78 °C with a nominal path length of 0.02 cm. The LiCN spectrum (5.0 mM) was measured at room temperature with a path length of 0.01 cm.

Results

Infrared Measurment. Although CuCN is insoluble in THF, it can be solubilized by addition of 2 equiv of LiCl. To simplify comparison, all cuprate IR measurements began with soluble CuCN·2LiCl. The low-temperature (−78 °C) IR spectra of CuCN·2LiCl (**1**), [MeCuCN]Li (**2**), and the solution prepared by addition of 2 equiv of MeLi to CuCN·2LiCl (**3**) are compared in Figure 1A. For solutions **1** and **2**, only a single ν_{CN} is observed at 2150 and 2133 cm^{-1}, respectively. In contrast, solution **3** has a strong absorption at 2115 cm^{-1} and a minor absorption at 2133 cm^{-1}. The latter disappears on addition of

(25) Becke, A. D. J. *J. Chem. Phys.* **1993**, *98*, 5648.
(26) Stevens, P. J.; Devlin, F. F.; Chablowski, C. F.; Frisch, M. J. *J. Phys. Chem.* **1994**, *98*, 11623.
(27) Hay, P. J.; Wadt, W. R. *J. Chem. Phys.* **1985**, *82*, 299.
(28) Dunning, T. H.; Hay, P. J. In *Modern Theoretical Chemistry*; W. Miller, Ed.; Plenum Press: New York, 1976; pp 1−28.
(29) Cui, Q.; Musaev, D. G.; Svensson, M.; Morokuma, K. *J. Phys. Chem.* In Press.

Table 1. Fitting Parameters of Cyanocuprates and LiCN[a]

sample	center (cm^{-1})	Gaussian function[b] width	height	area	Lorentzian function[c] width	height	area
1	2150	8.6	0.28	2.13	8	0.18	2.26
2	2133	8.8	0.31	2.42	5.2	0.30	2.45
3	2115	13.2	0.077	0.90			
LiCN/THF	2174				8.1	0.0045	0.057
	2178				4.0	0.0019	0.012

[a] Samples **1** and **2** were fit by a combination of Gaussian and Lorentzian functions. Sample **3** could be fit by a single Gaussian function. The two LiCN peaks were each fit by a Lorentzian function. [b] Gaussian = height × $\exp[-4(\nu - \nu_0)^2/\text{width}^2]$. [c] Lorentzian = height/$(1 + 4(\nu - \nu_0)^2/\text{width}^2)$).

a third equivalent of MeLi (CuCN·2LiCl + 3MeLi) suggesting that solution **3** is an equilibrium mixture of the cuprate species present in **2**, [MeCuCN]Li, and a new cuprate complex with $\nu_{CN} = 2115$ cm^{-1} (Figure 1). For comparison, the spectra for 5 mM LiCN in THF are also shown in Figure 1. The spectrum is dominated by a peak at 2174 cm^{-1} merging with a peak at 2178 cm^{-1}, together with a third, relatively weak band at 2068 cm^{-1}. In the following **1**, **2**, and **3** alone refer to the species that exhibit absorption at 2150, 2133, and 2115 cm^{-1}, respectively. Specifically, solutions **1**, **2**, and **3** refer to the THF solutions of CuCN·2LiCl, CuCN·2LiCl + MeLi, and CuCN·2LiCl + 2MeLi, respectively.

In contrast with the CN stretching frequencies, which decrease regularly from **1** to **2** to **3**, the integrated intensities of the 2150 and 2133 cm^{-1} peaks for **1** and **2** are comparable, while the 2115 cm^{-1} peak for **3** is both broader and much weaker. The estimated absorptivity of the 2115 cm^{-1} peak for **3** is comparable to that of the 2174 + 2178 cm^{-1} peaks in LiCN. The integrated intensities and peak widths are summarized in Table 1.

In order to characterize the CuCN + MeLi reaction more thoroughly, we measured titration curves for the addition of 0.2−2.2 equiv of MeLi to CuCN·2LiCl. Figure 2 shows the sequential IR spectra observed as **2** and **3** are produced from CuCN·2LiCl plus MeLi. From 0 to 1 equiv of MeLi (Figure 2, top), the 2133 cm^{-1} peak increases monotonically with a concomitant decrease in the 2150 cm^{-1} peak. In addition to these two major peaks, an additional weak absorption is observed at 2116−2120 cm^{-1} at intermediate MeLi concentration. There is no evidence for the 2116−2120 cm^{-1} peak at either of the end points for this portion of titration.

On further addition of MeLi (Figure 2, bottom) the intensity of the 2133 cm^{-1} peak for **2** decreases while the intensity of the 2115 cm^{-1} peak for **3** increases. In contrast to the earlier portion of the titration, the latter spectra show clear isosbestic behavior, indicating the presence of only two significant absorbing components in this spectral region. When exactly 2 equiv of MeLi have been added, a small peak at 2133 cm^{-1} remains. However, when 2.2 equiv or more of MeLi are added, the 2133 cm^{-1} species is completely converted to the 2115 cm^{-1} species.

For samples containing 0 or 1 equiv of MeLi, the IR spectra are consistent with the presence of only a single cyanide-containing species, while for intermediate stoichiometries, an additional cyanide-containing species is found. The areas of the 2150 and 2133 cm^{-1} peaks, normalized to unit absorbance at 0 MeLi (2150 cm^{-1}) and 1 MeLi (2133 cm^{-1}) are plotted in Figure 3. For comparison, the straight lines reflecting the idealized stoichiometric behavior **1** + MeLi → **2** are also shown. It is clear that there is significant negative deviation from stoichiometric behavior, as expected, since the cyanide-containing species observed at 2116−2120 cm^{-1} must be formed at the expense of either **1** (2150 cm^{-1}) or **2** (2133 cm^{-1}). From

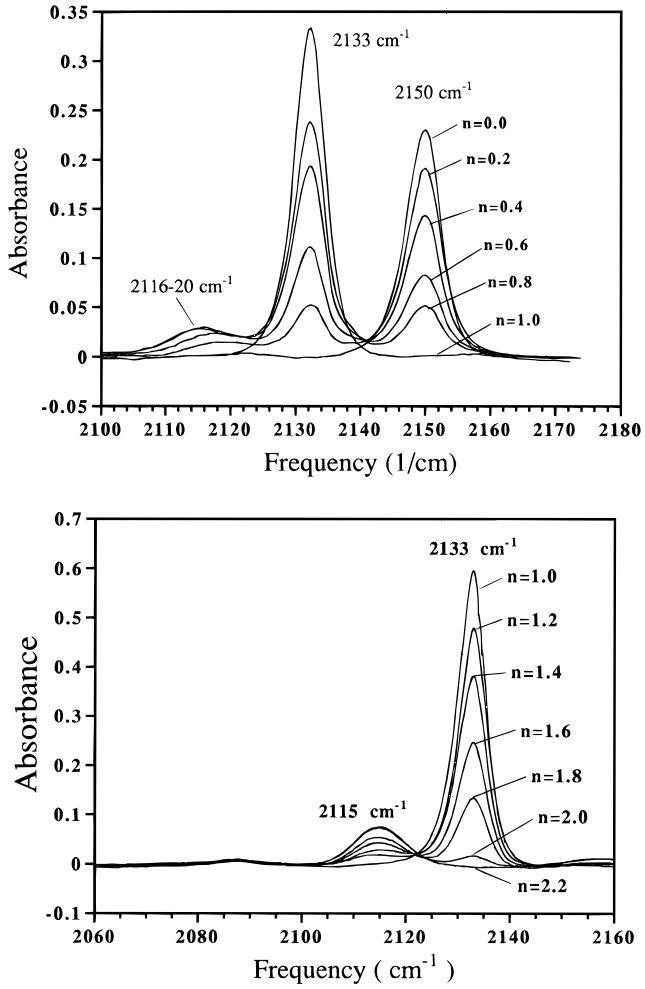

Figure 2. IR titrations for CuCN·2LiCl (**1**) + MeLi: (top) 0−1.0 equiv of MeLi; (bottom) 1.0−2.2 equi of MeLi. All spectra were measured at −78 °C with a nominal path length of 0.01 cm (A) or 0.02 cm (B).

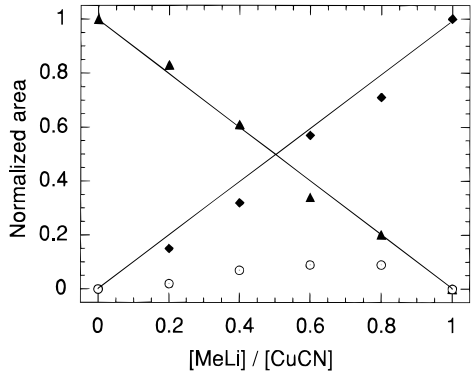

Figure 3. Normalized IR intensity of the 2150 cm^{-1} (▲) and 2133 cm^{-1} (◆) peaks of the spectra in Figure 2, top. Straight lines show expected dependence on [MeLi] for a stoichiometric reaction. Apparent concentration of CN^- that is not present in **1** or **2**, calculated by difference, is also shown (○).

Figure 3, it appears that the 2116−2120 cm^{-1} species comes mainly at the expense of the 2133 cm^{-1} species. To the extent that the absorption coefficients for the 2133 cm^{-1} and 2150 cm^{-1} bands are independent of [MeLi], the sum of the normalized absorbance should reflect the total molar percentage of cyanide that is present as **1** or **2**. The difference between this sum and 1.0 should be a measure of the fraction of cyanide that contributes to the 2116−2120 cm^{-1} band. This difference, which is also plotted in Figure 3, is less than 10% for all concentrations of MeLi. Since the area of the 2116−2120 cm^{-1}

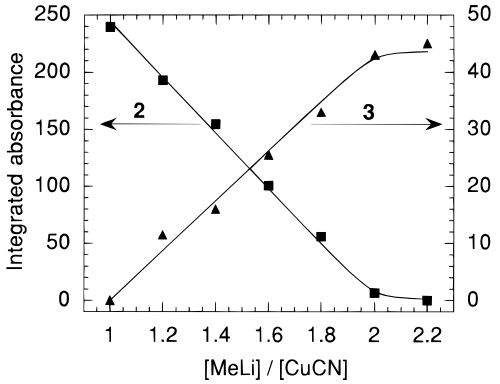

Figure 4. Integrated absorption of the 2133 cm^{-1} (■, left scale) and 2115 cm^{-1} (▲, right scale) peaks for the spectra in Figure 2, bottom. The lines represent the best fit to the equilibrium in eq A1 (see Appedix) with $K = 7.8 \times 10^3$ and absorption coefficients of $\epsilon = 2.4 \times 10^3$ (**2**) and 4.0×10^2 (**3**).

band is about 10% of the areas of the 2150 and 2133 cm^{-1} bands in solutions **1** and **2**, respectively, the absorption coefficient for the 2116−2120 cm^{-1} species must be comparable to or larger than those for **1** and **2**. The calculated molar absorption coefficient for the 2116−2120 cm^{-1} species ranges from 1.3×10^3 to 2.8×10^3 cm^{-2} M^{-1}.

The integrated absorption of the 2133 (**2**) and 2115 (**3**) cm^{-1} peaks are plotted vs [MeLi] in Figure 4. These data can be fit to an equilibrium between **2** and a new cyanocuprate **3** that absorbs at 2115 cm^{-1}:

$$\mathbf{2} + \text{MeLi} \rightleftharpoons \mathbf{3} \qquad (1)$$

The best fit of this equilibrium (see Appendix for fitting details) is shown in Figure 4. On the basis of this fit, the equilibrium constant in eq 1 is about 7.8×10^3 M^{-1}. This equilibrium constant is not, however, well-defined. Much larger values of *K* give comparable fits. Smaller values give somewhat worse fits but remain consistent with experimental uncertainties in the data down to $K \approx 1.5 \times 10^3$ M^{-1}.

Theoretical Computations. Geometry optimizations for **4**−**19** and other structures mentioned in the text were performed uniformly with the B3LYP/LANL2DZ protocol. Selected absolute energies (au) include: Me−Cu−CN−Li−OH, −412.93 367; **4**, −353.71 465; **5**, −260.70 118; **6**, −301.21 731; **7**, −487.11 754; **8**, −487.13 180; **9**, −623.24 986; **10**, −623.26 192; **11**, −487.10 955; **12**, −487.12 263; **13**, −536.84 381; **14**, −536.84 193; **15**, 536.84 199; **16**, −536.81 748; **17**, −536.80 892; **18**, −536.84 169.

In a number of cases, structures were optimized with and without water solvation at Li. A comparison of the corresponding ν_{CN} values demonstrates that water supplementation has only a minor influence on the calculated stretching frequency $\Delta\nu_{CN}$ in cm^{-1}: LiNC, +2; Me−Cu−CN−Li−OH_2, +5; **4**, −13; **5**, −16; **7**, −5; **8**, +25.

Normal coordinate analysis yielded zero imaginary frequencies with two exceptions. First, those structures with H_2O−Li functionalities mirrored across a plane of symmetry (e.g., **4** and **11**) generally showed two imaginary frequencies around −200 cm^{-1}. The latter are associated with the attempt of the water molecules to rotate H-atoms into the molecular plane. In all cases in the present work, the hydrogen atoms of each water molecule are constrained to lie symmetrically above and below the plane of any given cluster. This device permits first-shell "solvent" coordination at each lithium cation while minimizing unrealistic anion−HO interactions. Permitting the water molecules complete freedom during optimization causes them to relocate in the molecular plane near negatively charged centers. Not only does this promote inappropriate hydrogen bonding within the highly ionic cuprates but also other heavy-atom geometric distortions as well. Second, in addition to the negative water OH frequencies, constrained **18** displayed imaginary frequencies as it strained to move the exocyclic N-atom out of plane to return to **17**.

Table 2. Stretching Frequencies and Absorptivities for ν_{CN}

sample	solvent	ν_{CN}	K^a	ref
KCN	solid	2049		
CN^-	H_2O	2080	29	19
(TBA)CN	solid	2070		9
(TBA)CN	THF	2057		9
		2080		11
		2047, 2080	188	*c*
LiCN	solid	2095		11
LiCN	DMF	2079		9
LiCN	THF/HMPA	2068		12
	THF/DMF	2180		9
	THF	2068 (wk)		*c*
		2174/2178	480[b]	*c*
LiCN·LiI	THF	2110		11
CuCN	solid	2172		19
$Cu(CN)_2^-$	H_2O	2125	165	19
$Cu(CN)_3^{2-}$	H_2O	2094	1096	19
CuCN·2LiCl	THF	2150	1600	*c*
CuCN + MeLi	THF	2138		9
		2133	2400	*c*
CuCN + 2MeLi	THF	2130, 2109		12
		2138, 2118		7,9
		2128		11
		2115	400	*c*

[a] Integrated absorption coefficient in L mol^{-1}/cm^{-2}. [b] Based on integration of the combined 2174/2178 cm^{-1} bands. [c] Current work.

Discussion

IR Spectra. Several factors are known to affect ν_{CN} in metal cyanides.[22] Formation of strong σ bonds (e.g., in HCN(g)) results in increased ν_{CN}. Decreases in either the electronegativity or the oxidation state of the metal tend to cause a decrease in ν_{CN}.[21] The latter has been attributed to increased M(d) → CN(π^*) back donation,[23] while the increase in ν_{CN} on σ bond formation has been assigned to withdrawal of π^* electron density. Increases in metal coordination number typically lead to decreases in ν_{CN} in the range of 20−40 cm^{-1} for each added ligand. Additions of a metal to the nitrogen end of a coordinated cyanide may also result in increases in ν_{CN} by 20−40 cm^{-1}. This can be rationalized either by a simple kinematic model[20,22] or by variation in the electron density of the π orbital.[30]

The intensities of the cyanide stretch show even more dramatic dependence on structure. Ionic cyanide solutions (e.g. aqueous KCN) typically have very weak cyanide vibrations, with an integrated molar absorption[19] of less than 100 L mol^{-1} cm^{-2}. If cyanide is coordinated to a soft, polarizable metal (e.g. Cu(I)), the absorptivity increases by nearly an order of magnitude. Substitution effects can lead to further dramatic increases in absorptivity up to $\sim 10^3$ L mol^{-1} cm^{-2}, consistent with an increase in $d\mu/dQ$. M(d) → L(π^*) back bonding has been cited as a cause.[31] Similarly, formation of $M_1CN\cdots M_2$ bridges typically results in an increase in the absorptivity of the CN stretch. As discussed below, there are nonobvious exceptions to this rule.

Selected cyanide stretching frequencies and, where available, absorptivities are summarized in Table 2. Aqueous solutions

(30) Shriver, D. F. *J. Am. Chem. Soc.* **1963**, *85*, 1405.
(31) Overend, J. In *Infra-Red Spectroscopy and Molecular Structure*; M. Davies, Ed.; Elsevier Publishing Company: Amsterdam, 1963; pp 345.

of CN^- have ν_{CN} at 2080 cm^{-1}. Ionic salts of CN^- or solutions with noncoordinating cations (e.g., tetrabutylammonium) have similarly low ν_{CN} values in the range of 2047−2080 cm^{-1}. Solutions of LiCN measured in strongly coordinating solvents (e.g., HMPA), where the Li^+ should be complexed, also show low ν_{CN} frequencies (2068−2079 cm^{-1}). The ν_{CN} for LiCN in THF in the absence of strongly coordinating solvents is much higher (2174−2180 cm^{-1}), although there is also a small band at ∼2068 cm^{-1}. According to the DFT calculations, the higher frequency bands can be attributed to formation of Li^+/CN^- aggregates (e.g., **5** and **6**) in which the CN group is most likely bridging between Li atoms. The lower frequency band most likely represents either a terminal cyanide or even a "free" CN^-. This increase in ν_{CN} as a consequence of an Li···CN interaction is consistent with the behavior expected for formation of a σ bond to cyanide.

Solid CuCN shows a still higher ν_{CN} at 2172 cm^{-1}. This is consistent with the presence of Cu−CN−Cu structures in the solid. As expected, ν_{CN} decreases in mononuclear $Cu(CN)_2^-$ and decreases still further in the three-coordinate complex $Cu(CN)_3^{2-}$. Solution **1** (CuCN·2LiCl) shows a single ν_{CN} at 2150 cm^{-1} intermediate between CuCN(s) and $Cu(CN)_2^-$. This is consistent with our finding[13,15] that **1** contains linear [-Cu−CN−Cu-] aggregates with a Cu coordination number between 2 and 3. The observation of only a single, relatively narrow CN stretch in **1** demonstrates that the Cu/CN/Li/Cl aggregate(s), whose structure(s) remains to be determined, contain(s) only a single, well-defined cyanide environment. The theoretical calculations indicate that the vibrational frequencies of a few structures (**7**−**10**) with the formula CuCN·2LiCl are within ±30 cm^{-1} of the observed frequency. This suggests that the actual structure in solution is very close to these models. A full description is given in next section.

In general, there is reasonably good agreement between the ν_{CN} values that we observe and those reported previously. For measurements on comparable species, our values appear to be consistently 3−6 cm^{-1} higher than those reported by Oeschlager and coworkers[12] and 3−6 cm^{-1} lower than those reported by Lipshutz and coworkers.[7,9] In part, this may reflect instrumental differences. In addition, however, it appears that our spectra are significantly better resolved than earlier spectra, and thus part of the differences may be a consequence of better peak definition. The ν_{CN} values that we observe are used in the following discussion.

On addition of MeLi to form **2**, ν_{CN} decreases to 2133 cm^{-1}. This may be due solely to the loss of the distal Cu interaction as shown previously from EXAFS.[13,15] Alternatively, the decreases may reflect, in part, the substitution of a Me^- ligand for one of the CN^- ligands, since the more electron-releasing methyl group would be expected to lead to a decreased σ bonding from a geminal CN group. Addition of a second equivalent of MeLi results in a further decrease in ν_{CN}, although not to the extent seen in authentic three-coordinate Cu cyanides (Table 2). This is consistent with EXAFS results indicating that Cu remains two-coordinate in **3** and is probably not consistent with formation of a Me_2CuCN^{2-} species. The latter would be expected to have a much lower ν_{CN}, at least as low as that in $Cu(CN)_3^{2-}$ (2094 cm^{-1}), although the shortage of well-characterized mononuclear three-coordinate copper cyanides makes this comparison difficult. The frequency calculations support this contention, since the hypothetical copper three-coordinate cyanocuprate clusters **16** and **17** are predicted to show CN frequencies of 2035−2044 cm^{-1}.

More striking than the change in ν_{CN} is the dramatic *decrease* in molar absorptivity that is seen on formation of **3**. This is the opposite of the large *increase* in absorption that would be expected if the cyanide were present in a three-coordinate Cu complex. For example, the absorptivity increases nearly 7-fold on going from $Cu(CN)_2^-$ to $Cu(CN)_3^{2-}$. However, the 5-fold decrease in absorptivity between **2** and **3** is completely consistent with the displacement of CN^- from Cu in **3** to give a Li^+/CN^- aggregate such as **14**, described in the model calculation section. Recently, it has been proposed that the cyanide in **3** is coordinated to Cu in a side-on fashion.[11] In the absence of any well-characterized examples of such a structure, it is difficult to predict what ν_{CN} should be. However, since the Cu−CN interaction in such a structure is largely RCu → CN(π^*), it is likely that ν_{CN} would be at least as low as ν_{CN} in "free" CN^- (2080 cm^{-1}) and probably much lower.[32] Thus, this alternative structure seems inconsistent with the observed data.

Previous reports of the IR spectra for cyanocuprates have not been completely consistent, leading to the surprising conclusion that addition of either 1 or 2 equiv of MeLi to CuCN gives identical IR spectra. Particularly puzzling was the report[7] that the IR spectrum for "$Me(nBu)CuCN^{2-}$" is time dependent, despite the lack of time dependence in the NMR spectrum. The present titration data provide a resolution to these observations. From both Figures 1 and 2, it is clear that **2** and **3** do not have identical ν_{CN}. The 2115 cm^{-1} band, which was previously assigned as arising from one of two isomers of "Me_2CuCN^{2-}", comes in fact from the only cyanide species that is present when excess MeLi is added to CuCN. The 2133 cm^{-1} band, which was assigned to the other "Me_2CuCN^{2-}" isomer, is due instead to the residual [MeCuCN]Li that is present in solutions containing only 2 equiv of MeLi. The confusion in the original assignments may have arisen as a consequence of the nearly 5-fold greater integrated absorptivity and 50% narrower line width of the 2133 cm^{-1} band compared to that of the 2115 cm^{-1} band. These combine to give the 2133 cm^{-1} band a height comparable to that of the 2115 cm^{-1} band, even when the former is only present at less than 10% of the latter's concentration.

The titration curve for the conversion of **2** to **3** gives a formation constant for **3** of ∼7.8 × 10^3 M^{-1}. The curves of Figure 2 and the value of the formation constant make it clear that there are two different cuprate species in solution when only 2 equiv of MeLi are added to CuCN. For such an equilibrium mixture, minor variations in solution composition might shift the equilibrium significantly in favor of either **2** or **3**. This may explain the sensitivity of the CuCN + 2RLi reagent to additives such as BF_3 or HMPA.[12] Although two species are present in solution, only a single species was observed in the NMR.[7] Since the time scale for IR measurements is 10^4 to 10^{12} faster than for NMR,[33] the infrared observations imply a rapid equilibrium average in the NMR experiment.

In contrast to the **2** + MeLi ⇌ **3** equilibrium, there is no detectable CuCN·2LiCl present in solution when 1 equiv of MeLi has been added. A small amount of some new cyanide species absorbing at 2116−2120 cm^{-1} is formed at intermediate MeLi concentrations. However, as seen in Figure 3, this new species does not appear to represent more than 10% of the cyanide. With an apparent integrated absorptivity of ∼2 × 10^3, the 2116−2120 cm^{-1} species probably contains cyanide bound to Cu and is thus clearly different from the 2115 cm^{-1} species formed at high MeLi concentration. Since it appears to be formed at the expense of **2**, we suggest that it is some sort of Me−Cu−CN−Li_2X aggregate, formed for MeLi:CuCN ratios less than 1 (see below).

(32) Curtis, M. D.; Klingler, R. J. *J. Organomet. Chemistry* **1978**, *161*, 23−37.

(33) Muetterties, E. L. *Inorg. Chem.* **1965**, *4*, 769.

Normal Coordinate Analysis and Structure Assignment. In an effort to characterize the cyanide-containing species displaying the spectra of Figures 1 and 2, we have carried out geometry optimizations for a variety of structures using density functional theory combined with effective core potentials on copper. In many cases, water molecules were coordinated to lithium cations in the ionic aggregates to modulate the positive charge of the metal cation, as is the case in the first coordination sphere in solution. Each structure was subsequently subjected to normal coordinate analysis at the same level of theory to obtain the CN stretching frequencies. In general, the DFT formalism can provide equilibrium geometries, vibrational frequencies, and bond dissociation energies in excellent agreement with experiment.[34−36] With appropriate basis sets, accurate and unscaled vibrational frequencies are possible for small organometallics.[37] The nonlocal variation employed here (B3LYP) is no exception when applied to alkylcopper compounds. For example, B3LYP/LANL2DZ frequencies for CH_2N_2 and $Cu{\cdot}CH_2N_2$ have been shown to be accurate to within 4% of observed.[29] Thus, we take the present method to be capable of semiquantitative CN frequency determination at a minimum and to be useful for trend mapping and tentative structure assignment. As expected, CN stretching frequencies correlate well with CN bond lengths.

(A) Lithium Cyanide. Solutions of LiCN in THF show three cyanide bands at $\nu_{CN} = 2178$, 2174, and 2068 cm^{-1} (Figure 1, bottom), while matrix-isolated material (solid N_2, Ar, Ne) exhibits the same moiety at 2080−2084 cm^{-1}.[38,39] The simplest candidate structure is monomeric lithium isocyanide (LiNC), which is more stable than LiCN.[16] The calculated CN stretches for triatomic LiNC and the monosolvated species $H_2O{\cdots}$LiNC are 2050 and 2052 cm^{-1}, respectively, accommodating the lower experimental band within 20 cm^{-1}. The solvated dimer **4**, which has two coupled cyanide stretches of which the symmetric mode is infrared inactive, is an alternative structure. The asymmetric vibration in **4** is calculated to be at 2034 cm^{-1}. Although this is 34 cm^{-1} below the 2068 cm^{-1} band observed in THF, the dimer cannot be ruled out.

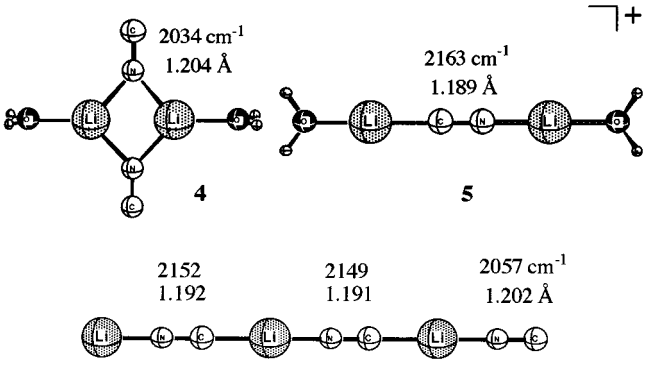

In general, higher frequency vibrations reflect tighter CN bonds. The solvate of dilithiated cyanide ($[Li{-}N{\equiv}C{-}Li]^+[CN]^-$, $\mathbf{5}^+[CN]^-$) is a possible source of higher frequency vibrations. Such a structure has been implicated in the NMR by treatment of LiCN with $LiClO_4$.[8] The calculated frequency $\nu_{CN} = 2163$ cm^{-1} fits the data nicely ($\Delta\nu_{CN} \leq 15$ cm^{-1}).

Finally, we consider the linear dimers $Li(NC{-}Li)_n{-}NC$ for $n = 1$ and 2. The structures show both inner and outer cyanides: ($n = 1$) $\nu_{CN} = 2145$ and 2055 cm^{-1}; ($n = 2$; **6**) $\nu_{CN} = 2152$, 2149, and 2057 cm^{-1}. These frequencies mimic the behavior of the simpler structures **4** and **5**, with a lower ν_{CN} for terminal cyanides and a higher ν_{CN} for internal cyanides. When the moderate polarity of THF is considered, **5**, with its charged cyanide, is likely to collapse to the neutral linear LiNC dimer. Consequently, the pattern of Figure 1, bottom, is most reasonably interpreted as arising from a mixture of linear (or zig-zag Li-solvated) LiNC oligomers with 2068 cm^{-1} end group cyanides and several similar but nonidentical internal cyanides appearing in the 2174−2178 cm^{-1} region.

(B) MeCu(CN)Li (2). This lower order cyano Gilman reagent is certainly linear, as are other representatives of the $[R{-}Cu{-}R']^-Li^+$ class.[37] As a result, the CN frequency has been modeled both by linear $[Me{-}Cu{-}CN]^-$, and by Me−Cu−CN−Li and Me−Cu−CN−Li−OH_2. The predicted ν_{CN} values, 2113, 2123, and 2128 cm^{-1}, respectively, are again within 20 cm^{-1} of the 2133 cm^{-1} value observed for **2** in THF.

(C) CuCN·2LiCl (1). Although the composition of **1** lends itself to considerable topological variation, it shows only a single cyanide stretch at 2150 cm^{-1} (Figure 1). Recently gathered EXAFS spectra suggest oligomerization.[15] We have considered various species that embody linear and cyclic themes. The simplest are the Gilman analogs of MeCu(CN)Li ($[Cl{-}Cu{-}CN]^-$ and Cl−Cu−CN−Li), structures yielding $\nu_{CN} = 2177$ and 2149 cm^{-1}, respectively. More complex linear aggregates are **7**−**10**.

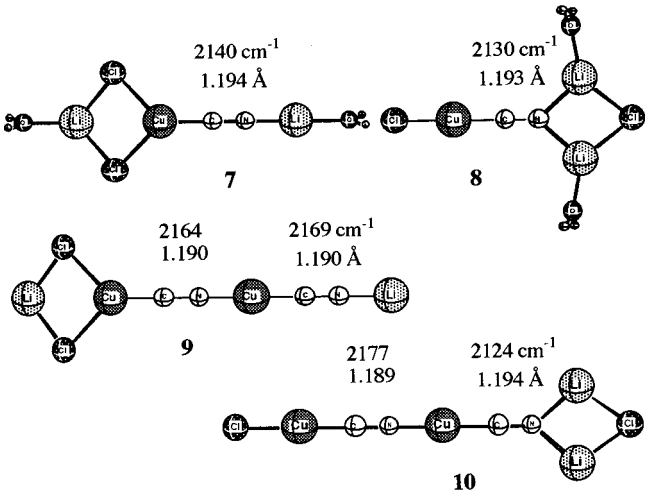

Clusters **7** and **8** correspond to the stoichiometric composition of **1**, while **9** and **10** incorporate an additional CuCN (i.e., $(CuCN)_2{\cdot}(LiCl_2)_2$). Species with bifurcated lithiation at N of CN deliver $\nu_{CN} = 2130$ (**8**) and 2124 (**10**) cm^{-1}. Divalent CN is calculated at 2140 (**7**), 2164, 2169 (**9**), and 2177 (**10**) cm^{-1}. The unweighted average of the six values is 2151 cm^{-1}. While the quantitative correspondence with the experimental value is certainly fortuitous, the family of structures is entirely consistent with EXAFS measurements, which suggested linear [-Cu−CN−Cu-] aggregates with a Cu coordination number between 2 and 3.[15]

Two additional cyclic structures with the $CuCN{\cdot}2LiCl = Cl_2$-$Cu(CN)Li_2$ composition (**11** and **12**) have been considered. These correspond to the lowest energy isomers calculated for cyanocuprates $R_2Cu(CN)Li_2$ (R = Me).[15−17]

(34) Johnson, B. G.; Gill, P. M.; Pople, J. A. *J. Chem. Phys.* **1993**, *98*, 5612.
(35) Andzelm, J.; Wimmer, E. *J. Chem. Phys.* **1992**, *96*, 1280.
(36) Eriksson, L. A.; Pettersson, L. G. M.; Siegbahn, P. E. M.; Wahlgren, U. *J. Chem. Phys.* **1995**, *102*, 872.
(37) Ricca, A.; Bauschlicher, C. W. *J. Phys. Chem.* **1994**, *98*, 12899.
(38) Ismail, Z. K.; Hauge, R. H.; Margrave, J. L. *J. Chem. Phys.* **1972**, *57*, 5137−42.
(39) Ismail, Z. K.; Hauge, R. H.; Margrave, J. L. *High Temp. Sci.* **1981**, *14*, 197−206.

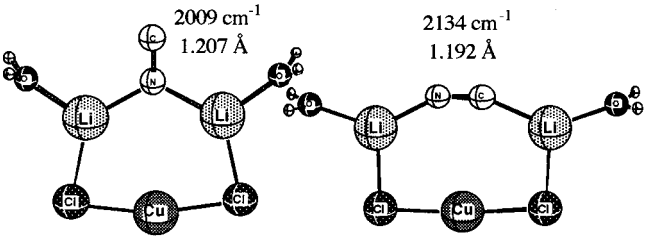

11 **12**

The C_{2v} entity **11** yields $\nu_{CN} = 2009$ cm^{-1}, somewhat too low to be considered a serious contributor to the 2150 cm^{-1} experimental band. Structure **12**, on the other hand, displays its CN stretch at 2134 cm^{-1}. It may well participate in the equilibrium mixture representing **1**.

(D) $Me_2CuLi\cdot LiCN$ (3). The species represented by this composition differs in a fundamental way from the previously considered structures. Namely, the presence of two methyl groups prevents the formation of linear structures such as **6**−**10**, since they can serve only as an end group or as the fulcrum of a nonlinear bridge between metal cations. While a variety of isomers have been proposed,[16] the two viable low-energy candidates are analogs of **11** and **12**, i.e., **13** with N−Li bonds and unsymmetrical **14**.[15,16]

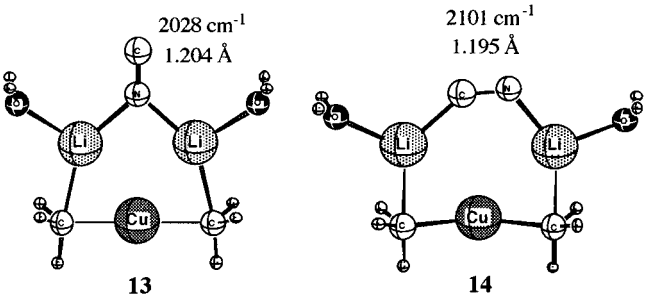

13 **14**

These structures provide $\nu_{CN} = 2028$ and 2101 cm^{-1}, respectively. Compared with the experimental value of 2115 cm^{-1} for **3**, that obtained for structure **14** makes it the clear favorite. An important feature of solution **3** is its 5-fold smaller absorptivity as compared with that of cyanocuprate **2**. In complete agreement with the latter observation, the calculated IR intensities for the cyano moieties in the corresponding structures are 398 (Me−Cu−CN−Li) and 22 (**14**) cm^{-1}. As previously described, the seven-membered cycle can be viewed as a relatively normal Gilman cuprate, [Me−Cu−Me]$^-$, bridged by the [Li−CN−Li]$^+$ cation.[16] Alternatively, the structure can be conceived as an analog of the Gilman dimer, $[Me_2CuLi]_2$, in which the two anions [Me−Cu−Me]$^-$ and CN$^-$ are linked by a pair of lithium cations.

Two additional structures are worthy of mention. The four-membered ring isomer **15** has been posited to be an energetic competitor of **13** and **14**.[16] It shows a calculated $\nu_{CN} = 2113$ cm^{-1}. While the latter matches the experimental value of **3** perfectly, **15** must be ruled out on the basis of the EXAFS result illustrating the absence of a Cu−CN bond.[15] Presumably, THF solvation favors **14** over **13** and **15**.

A discussion of the structure of $Me_2CuLi_2(CN)$ would be incomplete without considering a "higher order", trivalent copper structure as proposed by the authors of the earlier IR and NMR studies.[9,12,40] A reasonable candidate is the three-rung ladder **16**, in which the cyanide moiety of **13** ($r_{Cu-N} = 3.38$ Å) is inverted and the carbon is brought to within bonding distance

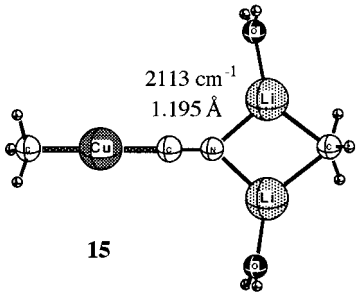

15

of the copper atom. Lithium diisopropylamide and LiCl have recently been shown to sustain such a structure by X-ray crystallography.[41] More elaborate ladders are also formed by lithium amides[42] and lithium phosphamides.[43] In the present case, tricoordinate cuprates have been estimated to be 15−22 kcal/mol less stable than **13** and to spontaneously revert to it.[16,17] Nonetheless, we have performed frequency calculations on the optimized structure of **16** with the Cu−C bond constrained to 2.33 Å. The resulting CN vibration falls at 2035 cm^{-1}, a full 80 cm^{-1} lower than the experimental value.

One of the problems associated with using water as a surrogate for ether solvents is the presence of polarized O−H bonds which tend to "drift" toward anionic centers. The C_{2v} structure **16** suffers from this problem in that the CN nitrogen rises 1.0 Å above the plane of rest of the molecule ($\theta_{N-C-Cu} = 146.7°$) as the lithiated waters twist to maximize the polar interaction ($r_{OH\cdots N} = 3.19$ Å). To attenuate the possible impact of the latter, the nitrogen was symmetrized to the plane of the molecule and the waters were adjusted to the torsional angles optimized for **11** to give **17** ($r_{OH\cdots N} = 3.79$ Å). The corresponding $\nu_{CN} = 2044$ cm^{-1} is still 77 cm^{-1} below the measured 2115 cm^{-1}, providing further evidence that neutral cuprate clusters incorporating trivalent Cu(I) are unsatisfying models for $Me_2CuLi_2(CN)$.

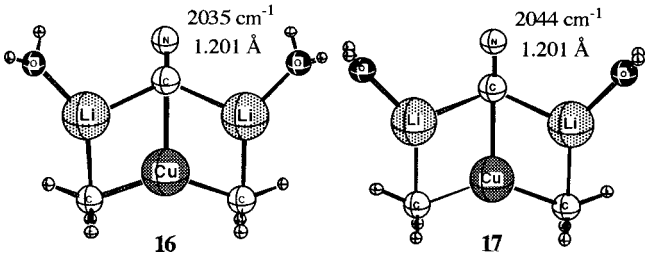

16 **17**

(E) The 2116−2120 cm^{-1} Species. Finally, in an attempt to provide a candidate for the species responsible for the transient and weak 2116−2120 cm^{-1} absorption at intermediate MeLi concentration (Figure 2, top), we have examined the properties of neutral aggregates of lithiated **2** and MX. For MX = CuCN and LiCl, this corresponds to [Me−Cu−CN−Li]·[CuCN] and [Me−Cu−CN−Li]·[LiCl], respectively. These constitutions could be formed from **2** and lead to **3** upon increasing MeLi concentration. Two linear structures ([Me−Cu−CN−Li−NC−Cu] and [Me−Cu−CN−Cu−CN−Li]) resulted in cyanide frequencies from 2140 to 2215 cm^{-1}, making them unlikely as candidate structures. Noteworthy, however, is that the latter is predicted to show $\nu_{CN} = 2155$ and 2168 cm^{-1}. These values can be compared with the cyanide stretch for solid CuCN at 2172 cm^{-1}. The spectrum of the [-Cu−CN−Cu-] unit is faithfully reproduced.

(40) Lipshutz, B. H.; Kozlowski, J. A.; Wilhelm, R. S. *J. Org. Chem.* **1984**, *49*, 3943−3949.

(41) Mair, F. S.; Clegg, W.; O'Neil, P. A. *J. Am. Chem. Soc.* **1993**, *115*, 3388.

(42) Mulvey, R. E. *Chem. Soc. Rev.* **1991**, *20*, 167.

(43) Driess, M.; Huttner, G.; Knopf, N.; Priotzkow, H.; Zsolnai *Angew. Chem., Int. Ed. Engl.* **1995**, *34*, 316.

The five-membered ring species **18** can be viewed as a [2 + 3] cycloadduct of the N−Li bond of [Me−Cu−CN−Li] and CuCN. Its ν_{CN} values fall at 2055 and 2068 cm^{-1}. These values appear too low to qualify as characterizing the intermediate observed at low MeLi concentrations. On the other hand, the 2105 cm^{-1} CN stretching frequency of four-membered ring **19**, a [2 + 2] adduct of N−Li and LiCl, matches the IR data within 10−15 cm^{-1}. The species likewise meets intuitive chemical requirements of intermediacy between **2** and **3**.

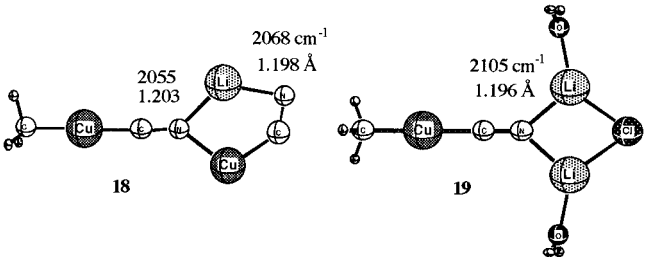

Factors Influencing Metal−Cyanide Stretching Frequencies. Copper(I) compounds contain metal−ligand bonds that are highly ionic.[17,44,45] According to natural population analysis (NPA),[46] the 10−20% covalency of the Cu−C bonds is strongly polarized toward carbon and composed primarily of s character.[44] On the basis of the NPA method, a recent study of the bonding in M−(C−X) complexes (M = Ag, Au; X = O, N), including M(CN)$_2^-$, concluded that M(d) → CO/CN(π*) back bonding is vanishingly small CX(π*) = <0.01−0.08 e).[47] A similar survey of Cu(I) cyanides came to the same conclusion.[48] In the present work, the reduction in CN stretching frequency from **1** to **2** (though not **3**) might reasonably be interpreted in terms of an increase in M(d) → π*(CN) back donation. NPA applied to structures **7** and **9** (models for **1**) demonstrates the presence of highly ionic Cu−C bonds and yields π*(CN) populations of 0.04−0.07 e. Me−Cu−CN−Li−OH$_2$, likewise, exhibits NPA π*(CN) populations of 0.05 e. In this framework, back bonding cannot explain the reduction in CN stretching from 2150 cm^{-1} in **1** to 2133 cm^{-1} in **2**.

Some insights into the origin of CN stretching frequency variations for structures such as **4**−**19** can be gained by first noting that gas phase, B3LYP/LANL2DZ CN$^-$ presents ν_{CN} = 1993 cm^{-1} as compared to 2050 cm^{-1} for CN−Li and 2163 cm^{-1} for **5**. The incremental 57 and 113 cm^{-1} $\Delta\nu$ increases, respectively, are directly associated with coordination of one and then two lithium cations to the linear, σ framework of the cyanide moiety by means of completely ionic bonds. The effects can be seen in a single structure by referring to **6**. Replacement of Li$^+$ with Cu$^+$ results in only minor perturbations in ν_{CN} as shown by the Cu−CN−Li (2169 cm^{-1}) and Cu−CN−Cu (2177 cm^{-1}) units of **9** and **10**, respectively. Tightening of the CN bond upon complexation of the σ lone pairs can be seen as a consequence of charge equalization. The metal cations serve to polarize the σ lone pairs along the molecular axis away from C and N. Cyanide π electrons compensate by contracting and localizing density between the same atoms. The importance of geometry as well as additional perturbations at lithium for this redistribution of electrons can be seen in the cyanide stretching registered by bridged **14** (2101 cm^{-1}). Here, ν_{CN} decreases by 62 cm^{-1} in comparison with that of acyclic **5**. Clearly, bridge formation in and of itself may not necessarily lead to higher CN frequencies, as proposed recently.[22]

As for the 17 cm^{-1} ν_{CN} drop from **1** to **2**, the collective structural set representing **1** (**7**−**10**) nicely illustrates the phenomenon that increased coordination at the metal ordinarily leads to a 20−40 cm^{-1} experimental fall in CN stretching frequency (**10** (Cl−Cu) → **7**/**9** (Cl$_2$−Cu); 2177 → 2164/2140 cm^{-1}). The increase in electron density around copper occasioned by the second chloride ion partly reverses the cationic σ drain mentioned above. Replacement of chloride with the very basic methyl group as in Me−Cu−CN−Li−OH$_2$ exaggerates the situation still further yielding ν_{CN} = 2130 cm^{-1}. The overall decrement between the **7**−**10** average (2151 cm^{-1}) and the latter ($\Delta\nu$ = 21 cm^{-1}) models the experimental drop quantitatively.

Conclusions

The disagreements in the cyanocuprate field have centered on the structure of the species formed from 2RLi + CuCN.[8,9,11−14,16,17] In a series of studies,[7,9,11] Lipshutz and coworkers have shown definitively that this mixture gives rise to a novel cyanide-containing species and that "free" LiCN is not formed. Our findings are in complete agreement with this conclusion. Moreover, our results indicate that there are only three dominant cyanocuprate species formed in solution. We formulate these as CuCN·2LiCl, MeCuCNLi, and Me$_2$CuLi$_2$CN. Lipshutz and coworkers have interpreted their results as indicating that a "higher order" Me$_2$CuCN^{2-} complex is formed.[7,9,11] Our results are inconsistent with this structure. The unique cyanide-containing species that is formed when the MeLi:CuCN ratio is >2.2 contains CN$^-$ in an environment that is most consistent with CN$^-$ interacting only with Li$^+$. Structure **14**[16,17] meets this requirement and also accommodates the unique, low-intensity CN stretching frequency at 2115 cm^{-1}.

Acknowledgment. Supported in part by funds from the University of Michigan, Office of the Vice President for Research. We thank Professor William Pearson and his group for help in preparation of some samples. J.P.S. is grateful to Professors Dennis Liotta and Keiji Morokuma (Emory University) for hospitality and generous support of this work.

Appendix

For the reaction

$$\mathbf{2} + \mathrm{MeLi} \rightleftharpoons \mathbf{3} \qquad \text{(A1)}$$

where **2** is MeCuCN·Li and **3** is "Me$_2$CuCN·Li$_2$", the equilibrium constant, *K*, is defined as

$$K = \frac{[\mathbf{3}]}{[\mathbf{2}][\mathrm{MeLi}]_{\mathrm{free}}} \qquad \text{(A2)}$$

If **2** is formed by the reaction,

$$\mathbf{1} + \mathrm{MeLi} \rightleftharpoons \mathbf{2} \qquad \text{(A3)}$$

then

$$[\mathrm{CuCN}] = [\mathbf{2}] + [\mathbf{3}] \qquad \text{(A4)}$$

by mass balance. If the ratio of MeLi that has been added to solution is R = [MeLi]/[CuCN], then the amount of free MeLi, [MeLi]$_{free}$, is given by R[CuCN] minus the [MeLi] used to form **2** and **3**:

(44) Böhme, M.; Frenking, G.; Reetz, M. T. *Organometallics* **1994**, *13*, 4237−4245.
(45) Antes, I.; Frenking, G. *Organometallics* **1995**, *14*, 4263−4268.
(46) Reed, A. E.; Curtiss, L. A.; Weinhold, F. *Chem. Rev.* **1988**, *88*, 899−926.
(47) Veldkamp, A.; Frenking, G. *Organometallics* **1993**, *12*, 4613−4622.
(48) Snyder, J. P. Manuscript in preparation.

$$[\mathrm{MeLi}]_{\mathrm{free}} = \mathrm{R}[\mathrm{CuCN}] - [\mathbf{2}] - 2[\mathbf{3}] \quad \text{(A5)}$$

Combining eqs A4 and A5 and eliminating [**2**] gives

$$[\mathrm{MeLi}]_{\mathrm{free}} = (\mathrm{R} - 1)[\mathrm{CuCN}] - [\mathbf{3}] \quad \text{(A6)}$$

Combining eqs A2, A4, and A6 gives a quadratic equation which can be solved for [**3**]

$$[\mathbf{3}] = \frac{[\mathrm{CuCN}]\mathrm{R}}{2} + \frac{1 - \sqrt{K^2[\mathrm{CuCN}]^2(\mathrm{R} - 2)^2 + 2K[\mathrm{CuCN}]\mathrm{R} + 1}}{2K} \quad \text{(A7)}$$

which means that, using (A4)

$$[\mathbf{2}] = (2 - \mathrm{R})\frac{[\mathrm{CuCN}]}{2} - \frac{1 - \sqrt{K^2[\mathrm{CuCN}]^2(\mathrm{R} - 2)^2 + 2K[\mathrm{CuCN}]\mathrm{R} + 1}}{2K} \quad \text{(A8)}$$

Integrated absorbance data for **2** and **3** were fit to eqs A8 and A7, respectively. Use of the nonlinear least-squares-fitting algorithm of the program Kaleidagraph to optimize K and the absorption coefficient for **2** resulted in values for K which were always greater than 1.5×10^3 M^{-1}. For **3**, K was less well-defined, with optimized values as large as 1×10^5 M^{-1}. For both **2** and **3**, the integrated absorption coefficients were well-defined as 2.4×10^3 and 4.0×10^2 cm^{-2} M^{-1}, respectively.

JA961862W